A Fixed Point Charge Model for Water Optimized to the Vapor−Liquid Coexistence Properties

Jeffrey R. Errington and Athanassios Z. Panagiotopoulos*

School of Chemical Engineering, Cornell University, Ithaca, New York 14853, and Institute for Physical Science and Technology and Department of Chemical Engineering, University of Maryland, College Park, Maryland 20742

Received: April 30, 1998

A new fixed-point charge potential model for water has been developed, targeting the accurate prediction of the vapor−liquid coexistence properties over a broad temperature range. The model consists of a Buckingham exponential-6 group at the oxygen center and a set of three point charges. The new model was designed primarily to reproduce coexisting vapor and liquid densities, vapor pressures, and critical parameters and secondarily the liquid structure of water at ambient conditions. To obtain an optimum set of intermolecular potential parameters, the Gibbs ensemble and histogram reweighting grand canonical Monte Carlo methods were used to test a large number of models that covered a wide range of parameter space. Recently developed Hamiltonian scaling grand canonical Monte Carlo techniques enabled us to move through parameter space in an efficient manner. Properties of the new model were determined over the temperature range of the liquid. Results were compared to the SPC, SPC/E, and MSPC/E models and to experimental data. The new model was found to be better than existing models for the coexistence densities, vapor pressures, critical parameters, and the second virial coefficient. It is inferior to the SPC/E and MSPC/E models in reproducing the dielectric constant. The oxygen−hydrogen and hydrogen−hydrogen radial distributions are in good agreement with experimental data; however, the second shell of the oxygen−oxygen radial distribution of the new model does not have the correct form.

Introduction

The phase behavior of water and aqueous mixtures plays a key role in biology, chemistry, physics, and the design of many chemical processes. Recent advances in simulation techniques have allowed calculation of phase equilibria of complex systems from detailed descriptions of intermolecular interactions. Implementation of these techniques to real fluids requires reliable intermolecular potential models for pure components. Due to the unique interactions in water, an intermolecular potential model valid over a broad range of densities and temperatures remains elusive. For technological applications such as separations, power generation, and environmental remediation, it is highly desirable to have a model that predicts vapor−liquid coexistence properties and the behavior of water at elevated temperatures and pressures. The focus of the present paper is on the development of such a model.

Fixed-point charge models of water are commonly used because of their simplicity and their successful description of the structure of liquid water at near-ambient conditions. A Lennard-Jones potential is usually used to describe the nonpolar forces in addition to a set of point charges to represent the polar interactions. Models of this type include the Bernal−Fowler,[1] ST2,[2] TIPS2,[3] TIP4P,[4] SPC,[5] SPC/E,[6] and a recently rescaled SPC/E model, MSPC/E.[7] Because most of these potentials were optimized to describe the liquid phase of water at ambient conditions, the models are inadequate at high temperatures. Most predict a critical temperature significantly below the experimental value.

Water is a highly polarizable molecule, with the effective dipole varying with temperature and density. Fixed-point charge models do not account for polarizability. A number of models have been introduced that account for polarizability. Dipole-polarizable models[8,9] account for polarizability by explicitly including the higher order electrostatic interactions (such as dipole−dipole, quadrupole−quadrupole, etc.). Although these models are more detailed than the fixed-point charge models, a significant improvement in the description of both the thermodynamic and structural properties has not been observed.[10] A drawback of these advanced models is the computation time required to calculate thermodynamic and structural properties. Computation time for Monte Carlo simulations of a dipole-polarizable model is at least 1 order of magnitude larger than a fixed-point charge model. The increased computational requirements of polarizable models do not permit, at the present time, optimizations of the type performed in the present paper.

An alternative to polarizable models is provided by "fluctuating charge" models,[11−13] which allow the point charges on atomic sites to respond to the local water environment, thus indirectly introducing polarizability. The fluctuating charge models have been shown to reproduce the liquid structure and dielectric properties better than fixed-point charge models; however, their ability to reproduce coexistence properties has not been studied in detail.[14] Although molecular dynamics simulations with fluctuating charge models require only slightly more CPU time than fixed-point charge models, Monte Carlo simulations are at least an order of magnitude slower. A new algorithm that reduces the CPU time for Monte Carlo simulations of fluctuating charge models has recently been introduced[15]

* To whom correspondence should be addressed at the University of Maryland. E-mail thanos@ipst.umd.edu.

S1089-5647(98)02068-9 CCC: $15.00
Published on Web 08/27/1998

and may provide a means for obtaining properties of fluctuating-charge models in the future.

Optimization of intermolecular potential model parameters to reproduce a given set of experimentally measured properties has not usually been performed in a systematic fashion in the past. The primary constraint is the amount of computer time required to evaluate accurately the properties of candidate models. Recent methodological advances allow for the evaluation of properties of multiple potential models from a single simulation and the extrapolation of properties measured at a certain set of thermodynamic conditions to different temperatures and densities.[16−21] One of the goals of the present paper is to illustrate how these techniques can be used to obtain optimized intermolecular potential parameters for a complex molecule such as water. An attractive alternative to fitting potential parameters to experimental data would be to obtain potential parameters from ab initio quantum mechanical calculations. Unfortunately, ab initio calculations cannot presently capture dispersion and many-body interaction effects present in liquids with accuracy comparable to that of empirical effective potentials. In a recent study, Liu et al.[13] proposed a new fluctuating-charge model for water by fitting potential parameters to ab initio data. The potential parameters pertinent to many-body interactions were adjusted to reproduce ab initio three-body energies of water trimers. Subsequently, potential parameters corresponding to pairs of molecules were adjusted to satisfy ab initio pair interaction energies. The new model was shown to be as successful in reproducing the liquid structure at ambient conditions as an empirically derived fluctuating-charge model.[12]

In this work, we have optimized a parameter set for a fixed-point charge model to describe accurately the saturated vapor and liquid densities, vapor pressures, critical parameters, and liquid structure of water. Initial work was performed using the Lennard-Jones potential to represent the nonpolar forces. However, after a lengthy search, no parameter set that could describe both thermodynamic properties and liquid structure could be located. In an attempt to determine an adequate model, a switch to the Buckingham exponential-6 potential[22] to describe the nonpolar interactions was made. The exponential-6 potential is more flexible than the Lennard-Jones potential, having three parameters instead of two. This added degree of freedom enabled us to find a parameter set that accurately describes the thermophysical properties of water, while giving a reasonable description of the liquid structure at ambient conditions.

The plan of the paper is as follows. We first describe the systematic approach taken in finding a new model and the methodologies used to calculate the properties of interest. We then present our results for the coexisting densities, vapor pressures, critical parameters, second virial coefficients, dielectric constants, and liquid structure of the new model. The results for the new model are compared to the SPC, SPC/E, and MSPC/E models and experimental data. The paper concludes with a discussion of the limitations of the proposed model and possible ways to address them in the future.

Model Development

In any optimization procedure a set of target properties to be optimized must first be defined. For this study, we have chosen as primary optimization objectives the saturated liquid and vapor densities as well as the vapor pressure, for temperatures from the triple point to the critical point. The structure of the liquid at ambient conditions was also taken into account in the optimization procedure. Coexisting densities and vapor pressures were found using both the Gibbs ensemble[23−25] and histogram reweighting grand canonical Monte Carlo.[26−28] Pair correlation functions were obtained from canonical ensemble[29] simulations. Critical parameters were determined by combining mixed-field finite-size scaling methods[30,31] with grand canonical Monte Carlo simulations. Recently developed Hamiltonian scaling grand canonical Monte Carlo techniques[21] were utilized to increase the efficiency of our search through parameter space.

Our first attempt at finding a new intermolecular potential model for water utilized a Lennard-Jones core.[32] Twenty different parameter combinations were studied using a methodology similar to the one for the exp-6 potential. The majority of our efforts were spent investigating a SPC type geometry; however, we did explore a geometry in which the negative charge was moved off the Lennard-Jones center toward the hydrogens on the dichotomy of the H−O−H angle (TIP4P type model). We also pursued models that utilized four point charges arranged in a tetrahedral geometry: two positive charges on the hydrogens and two negative charges on the lone pair electrons. Although a wide range of geometries and parameter space was explored, no acceptable set of parameters was found. At best, we were able to find a model that adequately described the vapor−liquid coexistence curve but did not provide a satisfactory description of the liquid structure at ambient conditions. For the optimized potential parameters,[32] the period of the radial distribution functions was considerably longer than that observed experimentally.

After concluding that the Lennard-Jones potential was not suitable, we turned to the Buckingham exponential-6 potential due to its greater flexibility. We kept the fixed-point charge representation of the polar interactions due to its computational tractability. An exponential-6 group was placed at the oxygen center along with a point charge of magnitude $-2q$. Two point charges, of magnitude $+q$, are placed a distance R from the oxygen center. The angle formed by the charges was fixed at a value of 109.5°. This combination leads to the following mathematical form for the interaction energy between two water molecules.

$$u(r) = \frac{\epsilon}{1 - 6/\alpha}\left[\frac{6}{\alpha}\exp\left(\alpha\left[1 - \frac{r}{r_m}\right]\right) - \left(\frac{r_m}{r}\right)^6\right] + \sum_{a=1}^{3}\sum_{b=1}^{3}\frac{1}{4\pi\epsilon_0}\frac{q_a q_b}{r_{ab}}, \quad \text{for } r > r_{max}$$

$$= \infty, \quad r < r_{max} \tag{1}$$

where ϵ, r_m, and α are exponential-6 parameters. Parameter r_m is the radial distance at which the exponential-6 potential is a minimum. The cutoff distance r_{max} is the smallest positive value for which $du_{exp-6}(r)/dr = 0$ and is obtained by iterative solution of eq 1. The reason a cutoff distance is required is that at very short distances the original Buckingham exponential-6 potential becomes negative. While canonical-ensemble Monte Carlo or molecular dynamics simulations never sample the unphysical attractive region, this is not the case on trial insertions in grand canonical simulations and particle transfers in Gibbs ensemble simulations. The radial distance for which $u_{exp-6}(r) = 0$, denoted by σ, can also be computed from eq 1. The value of r is the distance between two oxygen centers. The symbols q_a and q_b represent the value of the point charges on sites a and b, and r_{ab} is the distance between sites a and b.

TABLE 1: Intermolecular Potential Parameters for the Models Studied

model parameter	SPC	SPC/E	MSPC/E	new
nonpolar forces	LJ	LJ	LJ	exp-6
ϵ/k_B (K)	78.21	78.21	74.68	159.78
σ (Å)	3.167	3.167	3.116	3.195
α				12
q (e)	0.4100	0.4238	0.4108	0.3687
R	1.0	1.0	0.9839	1.0668
H−O−H angle (deg)	109.5	109.5	109.5	109.5
μ (D)	2.27	2.35	2.24	2.18

At the end of our search we decided that the model presented in Table 1 best reproduced the observable quantities of interest. It was found that the value of r_{max}, calculated by finding the smallest radial distance for which $du_{exp-6}/dr = 0$, was too small. If a positive charge was randomly placed close to a negative charge, the magnitude of the Coulombic energy would be greater than the exponential-6 energy, causing the molecules to stick together unrealistically. This occurred during particle transfers and large particle displacements in the vapor phase. The energy barrier for a positive charge to penetrate into the exponential-6 core was very large. The probability of crossing the energy barrier was less than 1 in 10^{85}. To overcome this simulation artifact, the value of r_{max} was set to 1.75 Å.

The mathematical model of eq 1 contains five parameters: ϵ, σ, α, q, and R. To determine an optimum parameter set, the following procedure was performed for 17 potential models that covered a wide range of parameter space.

1. Five parameters were selected.

2. A grand canonical Monte Carlo simulation was performed at near critical conditions.

3. The critical temperature and density were determined using mixed-field finite-size scaling techniques.

4. The model parameters were rescaled using corresponding states to match the critical temperature of the model to the experimental critical temperature of real water.

5. A Gibbs ensemble simulation at a temperature of 300 K was performed.

6. Again, the model parameters were rescaled using corresponding states to match the saturated liquid density of the model to the experimental saturated liquid density at a temperature of 300 K.

7. A canonical ensemble simulation at a temperature of 300 K and density of 1.0 g/cm^3 was performed.

8. A Gibbs ensemble simulation at a temperature of 450 K was performed.

The above procedure forced each of the models tested to have the experimental value for the critical temperature and saturated liquid density at 300 K. This provided a common reference point for all models and increased the efficiency of the optimization procedure. The final parameters of each model were compared, and the thermodynamic and structural properties for each model were obtained. Although the numerical partial derivatives of properties with respect to model parameters could not be determined with high accuracy, qualitative trends were found. It was observed that the saturated liquid densities at 450 K changed relatively little among the different parameter sets. Conversely, it was determined that the saturated vapor densities and vapor pressures varied by a relatively large amount between potential models. All three of the charge radial pair distribution functions (negative−negative, negative−positive, positive−positive) were observed to be sensitive to small changes in the model parameters. The details of all 17 models examined are available as supplementary material from the author.[32]

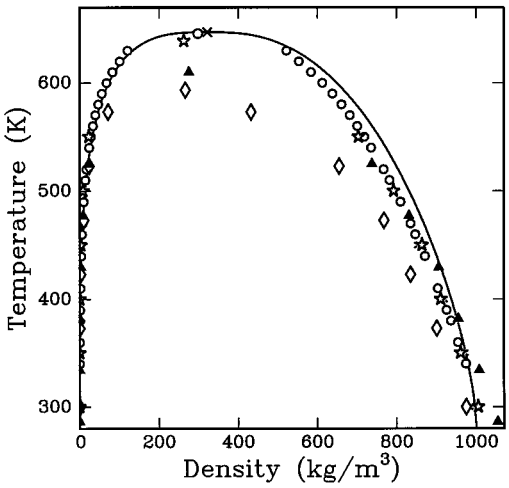

Figure 1. Phase diagram of water. The circles represent calculations for the new model using GCMC. Diamonds, stars, triangles, and asterisks represent GEMC calculations for the SPC, SPC/E, MSPC/E, and new models, respectively. A solid line is used for experimental data and a cross for the experimental critical point.

Hamiltonian scaling grand canonical Monte Carlo (HSGCMC) was found to be a useful tool in this study. It allowed for a quick transition from one potential model to the next. As an illustration of how this method is implemented, let us imagine a previously examined model (model 1) with parameters ϵ_1 and q_1. It is desired to increase the value of ϵ while keeping the critical temperature of the model fixed at the experimental value by increasing the value of q. A HSGCMC run would be completed, with model 1 and three trial potential models, at the critical temperature of model 1. The three trial models would all have a new value of the energy parameter, ϵ_2, with different values for the partial charge, q_{2a}, q_{2b}, and q_{2c}. The values of the charges would be selected such that the critical temperatures of the three trial models bracketed the experimental critical temperature of water. The appropriate value of q would then be determined from a linear interpolation of the three trial potential models. This would remove the time-consuming steps 2−4 above.

Results and Discussion

Phase Behavior. The coexistence curve for water is shown in Figure 1. The uncertainties for the calculations are not shown to make the plot more readable; however, all of the uncertainties can be obtained from the supplementary material.[32] On average, the Gibbs ensemble calculations for the saturated liquid densities are accurate to 2% and the vapor densities to 20%. The saturated liquid densities of the new model and the SPC/E model are consistently lower than the experimental values,[33] with an average error of 2.7% over the temperature range 300−550 K. The SPC model predictions are considerably lower than experimental values, with an average deviation of 11.8%. The MSPC/E model underpredicts the saturated liquid densities at higher temperatures and overpredicts at lower temperatures with an average error of 3.1%. For the saturated vapor densities, the new, SPC, and MSPC/E models are all in good agreement with experimental values at lower temperatures; however, the vapor densities of the SPC and MSPC/E models deviate significantly at higher temperatures. The vapor densities of the SPC/E model are consistently a factor of 2 lower than experimentally observed.

TABLE 2: Critical Parameters of the Models Studied

model	T_c (K)	ρ_c (kg/m^3)	P_c (bar)
SPC	593.8 ± 1.2	271 ± 6	129 ± 2
SPC/E	638.6 ± 1.5	273 ± 9	139 ± 4
MSPC/E	609.8 ± 1.4	287 ± 9	139 ± 4
new	645.9 ± 1.1	297 ± 5	183 ± 3
expt	647.1	322.0	220.6

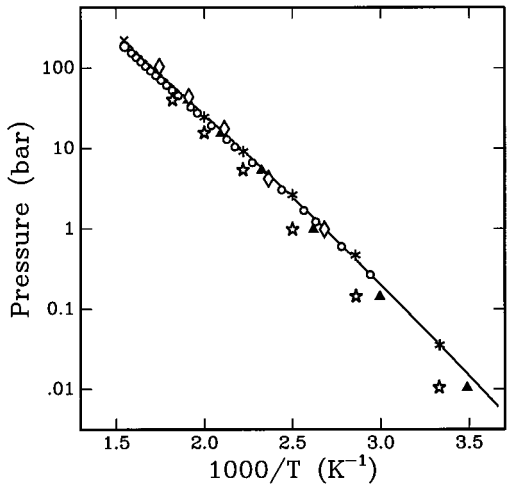

Figure 2. Vapor pressure of water. Symbols are the same as for Figure 1.

The critical parameters of the models are presented in Table 2. The critical temperatures and densities were found from a mixed-field finite-size scaling analysis[30,31] on histograms that were collected during grand canonical Monte Carlo runs at near critical conditions. The critical pressures were calculated by extrapolating the vapor pressure curve, found using histogram reweighting,[21] to the critical temperature. The critical temperatures and densities of the SPC and SPC/E models are consistent with values we reported in an earlier communication.[34] The values for the critical temperatures are in reasonably good agreement with previously reported values;[7,35−37] however, the critical densities are slightly lower than values calculated from earlier studies. These differences can be explained by the fact that earlier studies determined the critical density from an extrapolation of the rectilinear diameter where as we did not have to assume the validity of the law of rectilinear diameters.

The critical temperature of the new model is within 0.2% of the experimental value,[33] with the SPC/E model being only slightly worse at 1.3%. The SPC and MSPC/E models predict critical temperatures significantly lower than the experimental value. The critical densities of all the models are too low. The new model is the closest, followed by the MSPC/E model, and then the SPC/E and SPC models. Similar to the critical densities, the critical pressures of all the models are too low. Again, the new model is the closest, followed by the SPC/E and MSPC/E models, and then the SPC model.

Vapor Pressure. The vapor pressure of water is shown in Figure 2. The new, SPC, and MSPC/E models are all in reasonable agreement with experimental values.[33] The new model underpredicts vapor pressures near the critical point by a maximum of 17%, with agreement improving at lower temperatures. The SPC/E model vapor pressure curve is consistently a factor of 2 lower than the experimental value, an unacceptably large deviation for many applications.

Second Virial Coefficient. The second virial coefficient is an important parameter for determining the thermodynamic properties of the vapor phase. The second virial coefficients of the new model were calculated using histogram reweighting techniques. The virial expansion truncated after two terms is

$$Z = 1 + B/V \tag{2}$$

where Z is the compressibility factor, B is the second virial coefficient, and V is the specific volume. A grand canonical Monte Carlo simulation was performed in the gas phase. The histogram collected was then reweighted for a series of chemical potentials to accumulate $P-V-T$ data along the isotherm for which the simulation was run. The second virial coefficient was then identified as the slope of a plot of $Z - 1$ versus $1/V$. The method was verified by calculating the second virial coefficient at several temperatures for the SPC/E model. Our results were in very good agreement with those of Guissani and Guillot.[36]

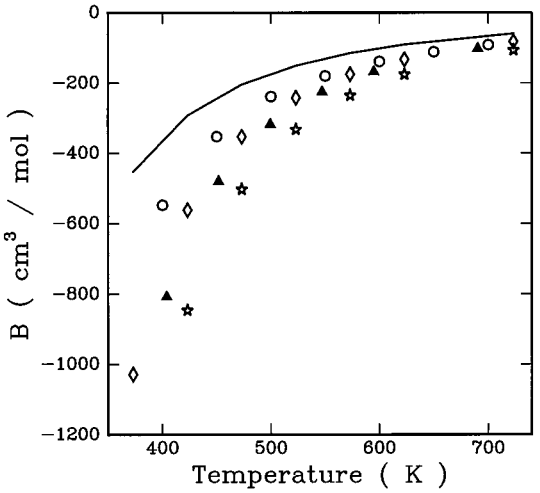

Figure 3. Second virial coefficient of Water. Diamonds, stars, triangles, and circles are used for the SPC, SPC/E, MSPC/E, and new models, respectively. A solid line is used for experimental data.

The second virial coefficient of water is displayed in Figure 3. The results for the new model were calculated from the method described above. The results for the SPC and SPC/E models were taken from ref 36. The trend shown in Figure 3 is not surprising, considering the bare dipole moment of water in the gas phase, 1.85 D. The dipole moments of all models are significantly higher than the gas-phase dipole moment of real water, causing a large discrepancy between model predictions and experimental data.[38] The agreement with experimental data is best for the new model which has the lowest dipole moment, $\mu = 2.18$ D, and worst for the SPC/E model which has the highest dipole moment, $\mu = 2.35$ D.

Dielectric Constant. The large dielectric constant of water is one of its most interesting properties, with implications in biology, solution chemistry, and the study of electrolytes. When the long-range electrostatic interactions are calculated with the Ewald summation,[39,40] as is the case for our simulations, the dielectric constant, ϵ, is given by

$$\epsilon - 1 = (4\pi/3)\langle \mathbf{M}^2 \rangle \beta\rho \tag{3}$$

where $\mathbf{M}$ is the total dipole moment of the simulation box ($\mathbf{M} = \sum_i \mu_i$), β is the reciprocal temperature, and ρ is the density. The quantity $\langle \mathbf{M}^2 \rangle$ is a slowly fluctuating quantity, and thus the accumulation of this average has to be performed over very long simulation runs. Our calculations of the dielectric constant were determined from canonical ensemble Monte Carlo simulations. At temperatures of 300 and 350 K a total of 200 million configurations were used to determine the dielectric constant.

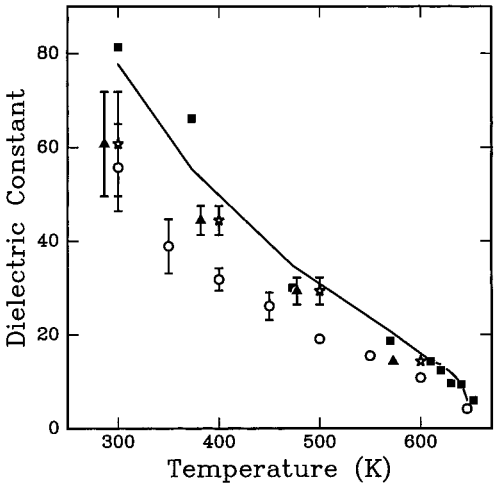

Figure 4. Dielectric constant of water. The solid squares represent calculations from ref 36 for the SPC/E model. The rest of the symbols are the same as for Figure 3.

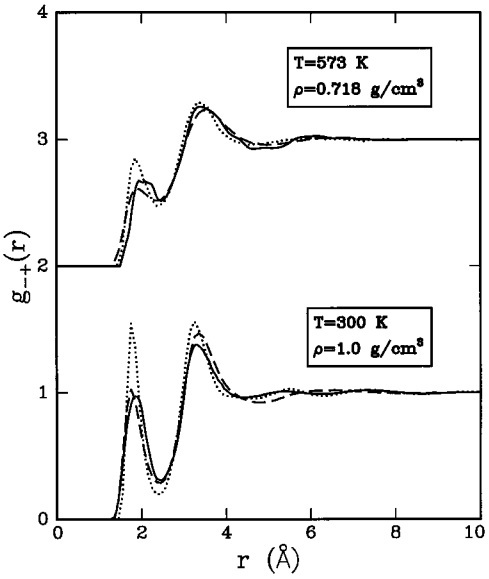

Figure 5. Positive−negative pair correlation function. Dashed and dotted lines are used to represent the new and SPC/E models, respectively. A solid line is used for experimental data for the hydrogen−oxygen pair correlation function.[42]

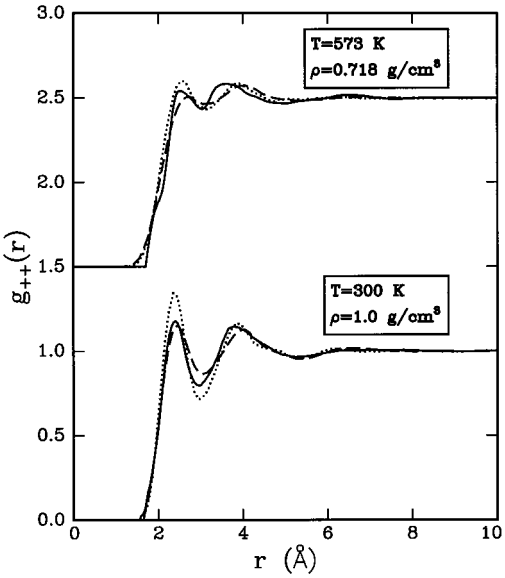

Figure 6. Positive−positive pair correlation function. Symbols are the same as in Figure 5.

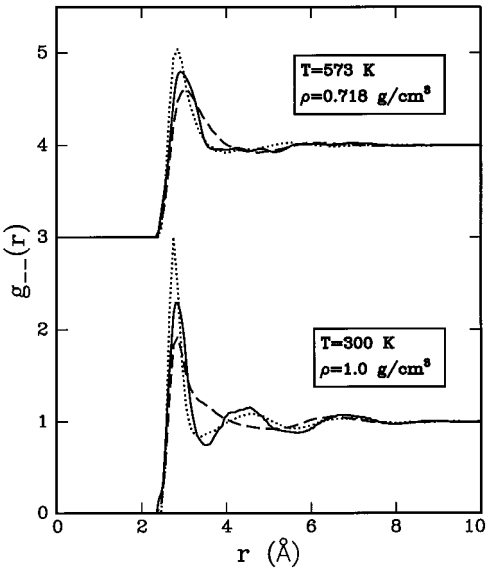

Figure 7. Negative−negative (oxygen−oxygen) pair correlation function. Symbols are the same as in Figure 5.

For all other temperatures, 100 million production steps were used to calculate the averages.

The dielectric constant of water is displayed in Figure 4. The agreement between our results and those of Guissani and Guillot,[36] for the SPC/E model, is good at higher temperatures; however, there are notable differences at lower temperatures. These differences can be attributed to the large uncertainties in calculations of the dielectric constant. The SPC/E model is in much better agreement with experimental data[41] than the new model. The reason for this is twofold. The dielectric constant is closely related to the dipole−dipole correlations at long distances. The degree to which the molecules are correlated over long distances can be determined from the Kirkwood factor, G_k, which is given by

$$G_k = \langle \mathbf{M}^2 \rangle / N\mu^2 = \sum_i^N \langle \mathbf{u}_t \cdot \mathbf{u}_i \rangle \qquad (4)$$

where $\mathbf{u}_i$ is a unit vector collinear to the dipole moment of μ_i of the molecule i and t is a test molecule in the system. We found that the Kirkwood factor for the SPC/E model was consistently larger than the new model, indicating that the SPC/E molecules correlate more at long distances than molecules interacting via the new potential. The second factor causing the dielectric constant of the SPC/E model to be larger than the new model is the magnitude of the bare dipole moment. The dielectric constant is approximately proportional to the square of the dipole moment. The dipole moment of the SPC/E model is 8% larger than the new model, which if all other things were equal would cause approximately a 16% difference in the dielectric constant.

Liquid Structure. The exact position of the hydrogen nucleus is undefined in the proposed model—only the position of the centers of positive charge is specified. However, we assume that we can approximate the position of the hydrogen nucleus with the center of positive charge. The pair correlation function between the sites of the positive and negative charge, g_{-+}, is shown in Figure 5 for ambient conditions and a

temperature of 573 K and density of 718 kg/m^3. It is observed that under both conditions the new model and the SPC/E model correctly predict the position of the peaks relative to experimental data;[42] however, the new model predicts the magnitude of the peaks significantly better than the SPC/E model. The positive−positive pair correlation function is displayed in Figure 6. Again, it is clear that the new model predicts the magnitude of the peaks more accurately than SPC/E, with both models predicting roughly the correct position of the peaks. The negative−positive and positive−positive pair correlation functions give some indication as to how well the model describes hydrogen bonding, an important interaction in water. The negative−negative (oxygen−oxygen) pair correlation function is shown in Figure 7. At ambient conditions the new model and SPC/E model both predict the position of the first peak; however, the form of the second shell of the distribution function is not predicted correctly by the new model.

Conclusions

We have optimized an intermolecular potential model for water that consists of a Buckingham exponential-6 core and fixed-point charges. The model was optimized to reproduce the coexisting densities, vapor pressure, critical parameters, and liquid structure at ambient conditions using a variety of simulation techniques. For each of several models tested, parameters were rescaled to match the model critical temperature and saturated liquid density at 300 K to the corresponding experimental values. The critical temperature, critical density, and liquid structure along with the vapor pressure and coexisting densities at 300 and 450 K were calculated to provide an overview of each model. Hamiltonian scaling grand canonical Monte Carlo was found to be a useful tool in making a transition from one parameter set to the next.

A new model was found that significantly improves the description of water over current fixed-point charge models. The new model reproduces the critical temperature to within 0.2%, the critical density to within 8%, and saturated liquid densities to within an average of 2.5%. Vapor pressures are also in good agreement with experiment. The model second virial coefficient is in better agreement with experiment than other fixed-point charge models. However, the dielectric constant is not in as good of agreement with experimental data as the SPC/E and MSPC/E models. The negative−positive and positive−positive radial distribution functions are in better agreement with experiment than current models, but the new model does not describe correctly the second shell of the negative−negative radial distribution function.

We feel that the new model will be applicable to the study of separations, environmental remediation, and biological systems. The model has an advantage over other models in that it reproduces accurately the vapor pressure, and thus the chemical potential in mixtures, to high temperatures. This property would be very useful for modeling supercritical water oxidation processes. Due to the poor description of the dielectric constant, the new model may not be useful for the study of electrolytes. Allowing the magnitude of the charges to respond to the local environment has been shown[12,13] to improve the dielectric constant. The addition of fluctuating charges to the new model may be a significant improvement. With new algorithms being developed to reduce the CPU time for fluctuating charge models, an optimization procedure similar to the one used in this paper may be possible in the near future.

Acknowledgment. Financial support for this work has been provided by the National Science Foundation, under Grant CTS-9509158. Computational resources were provided in part by the Cornell Theory Center.

References and Notes

(1) Bernal, J. D.; Fowler, R. H. *J. Chem. Phys.* **1993,** *97*, 13841.

(2) Stillinger, F. H.; Rahman, A. *J. Chem. Phys.* **1974,** *60*, 1545.

(3) Jorgensen, W. L. *J. Chem. Phys.* **1982**, *77*, 4156.

(4) Jorgensen, W. L.; Chandrasekhar, J.; Madura, J. D.; Impley, R. W.; Klein, M. L. *J. Chem. Phys.* **1983**, *79*, 926.

(5) Berendsen, H. J. C.; Postma, J. P. M.; van Gunsteren, W. F.; Hermans, J. In *Intermolecular Forces*; Pullman, B. Ed.; Reidel: Dordrecht, Holland, 1981.

(6) Berendsen, H. J. C.; Grigera, J. R.; Straatsma, T. P. *J. Phys. Chem.* **1987**, *91*, 6269.

(7) Boulougouris, G. C.; Economou, I. G.; Theodorou, D. N. *J. Phys. Chem. B* **1998,** *102*, 1029.

(8) Kozack, R. E.; Jordan, P. C. *J. Chem. Phys.* **1992**, *96*, 3120.

(9) Chialvo, A. A.; Cummings, P. T. *Fluid Phase Equilib.***,** in press.

(10) Kiyohara, K.; Gubbins, K. E.; Panagiotopoulos, A. Z. *Mol. Phys.*, in press.

(11) Wallqvist, A.; Teleman, O. *Mol. Phys.* **1991**, *74*, 515.

(12) Rick, S. W.; Stuart, S. J.; Berne, B. J. *J. Chem. Phys.* **1994**, *101*, 6141.

(13) Liu, Y. P.; Kim, K.; Berne, B. J.; Friesner, R. A.; Rick, S. W. *J. Chem. Phys.* **1998,** *108*, 4739.

(14) Medeiros, M.; Costas, M. E. *J. Chem. Phys.* **1997**, *107*, 2012.

(15) Martin, M. G.; Chen, B.; Siepmann, J. I. *J. Chem. Phys.* **1998**, *108*, 3383.

(16) Torrie, G. M.; Valleau, J. P. *J. Comput. Phys.* **1997,** *23*, 187.

(17) Torrie, G. M.; Valleau, J. P. *J. Chem. Phys.* **1977**, *66*, 1402.

(18) Valleau, J. P. *J. Comput. Phys.* **1991**, *96*, 193.

(19) Valleau, J. P. *J. Chem. Phys.* **1993,** *99*, 4718.

(20) Kiyohara, K.; Spyriouni, T.; Gubbins, K. E.; Panagiotopoulos, A. Z. *Mol. Phys.* **1996**, *89*, 965.

(21) Errington, J. R.; Panagiotopoulos, A. Z. *J. Chem. Phys.* **1998,** *109*, 1093.

(22) Buckingham, R. A. *Proc. R. Soc. London* **1938**, *168A*, 264.

(23) Panagiotopoulos, A. Z. *Mol. Phys.* **1987,** *61*, 813.

(24) Panagiotopoulos, A. Z.; Quirke, N.; Stapleton, M.; Tildesley, D. J. *Mol. Phys.* **1988,** *63*, 527.

(25) Smit, B.; de Smedt, P.; Frenkel, D. *Mol. Phys.* **1989,** *68*, 931.

(26) Ferrenberg, A. M.; Swendsen, R. H. *Phys. Rev. Lett.* **1988**, *61*, 2635.

(27) Ferrenberg, A. M.; Swendsen, R. H. *Phys. Rev. Lett.* **1989**, *63*, 1195.

(28) Panagiotopoulos, A. Z.; Wong, V.; Floriano, M. A. *Macromolecules* **1998,** *31*, 912.

(29) Frenkel, D.; Smit, B. *Understanding Molecular Simulation*; Academic Press: London, 1996.

(30) Wilding, N. B.; Bruce, A. D. *J. Phys.: Condens. Matter* **1992**, *4*, 3087.

(31) Wilding, N. B. *Phys. Rev. E* **1995**, *52*, 602.

(32) Unpublished data, available from http://thera.umd.edu/jerring/water.

(33) NIST Chemistry WebBook, http://webbook.nist.gov/chemistry.

(34) Errington, J. R.; Kiyohara, K.; Gubbins, K. E.; Panagiotopoulos, A. Z. *Fluid Phase Equilib.*, in press.

(35) de Pablo, J. J.; Prausnitz, J. M.; Strauch, H. J.; Cummings, P. T. *J. Chem. Phys.* **1990**, *93*, 7355.

(36) Guissani, Y.; Guillot, B. *J. Chem. Phys.* **1993**, *98*, 8221.

(37) Alejandre, J.; Tildesley, D. J.; Chapela, G. A. *J. Chem. Phys.* **1995**, *102*, 4574.

(38) Tsonopoulos, C.; Heidman, J. L. *Fluid Phase Equilib.* **1990**, *57*, 261.

(39) De Leeuw, S. W.; Perram, J. W.; Smith, E. R. *Proc. R. Soc. London* **1980**, *A373*, 27.

(40) Heyes, D. M. *J. Chem. Phys.* **1981**, *74*, 1924.

(41) Haar, J.; Gallagher, J. S.; Kell, G. S. *NBS/NRC Steam Tables;* Hemisphere: Washington, DC, 1984.

(42) Soper, A. K.; Turner, J. *Int. J. Mod. Phys. B* **1993**, *7*, 3049.